PHYSICAL REVIEW LETTERS

Molecular Beam Collisions with a Magnetically Trapped Target

Brian C. Sawyer, Benjamin K. Stuhl, Dajun Wang, Mark Yeo, and Jun Ye

JILA, National Institute of Standards and Technology and the University of Colorado
Department of Physics, University of Colorado, Boulder, Colorado 80309-0440, USA

Cold, neutral hydroxyl radicals are Stark decelerated and efficiently loaded into a permanent magnetic trap. The OH molecules are trapped in the rovibrational ground state at a density of $\sim 10^6$ cm^{-3} and temperature of 70 mK. Collision studies between the trapped OH sample and supersonic beams of atomic He and molecular D_2 determine absolute collision cross sections. The He-OH and D_2-OH center-of-mass collision energies are tuned from 60 cm^{-1} to 230 cm^{-1} and 145 cm^{-1} to 510 cm^{-1}, respectively, yielding evidence of quantum threshold scattering and resonant energy transfer between colliding particles.

Research in the field of cold polar molecules is progressing rapidly. An array of interesting topics is being developed, including precision measurement and fundamental tests [1–3], quantum phase transitions [4], and ultracold chemistry [5,6]. In particular, dipolar molecules with well-defined quantum states will enable us to exquisitely control their interactions via applied electric fields [7,8]. The long-range, anisotropic interactions between dipolar molecules lead to new types of collision dynamics that could be used for novel collective effects [9,10], quantum state engineering, and information processing.

Ultracold heteronuclear molecules have been produced via magnetic association or photoassociation of dual-species ultracold atom pairs [11,12]. Most of these molecules are in excited rovibrational states, permitting ultracold atom-molecule collision studies to probe molecular decay processes [13,14]. Coherent control techniques via exquisite manipulation of light fields have been implemented to drive these internally excited molecules produced in the initial association step into deeply bound states with large dipole moments [15,16].

Cold polar molecules in the ground state can be directly produced via cryogenic buffer-gas cooling or Stark deceleration, but at temperatures typically in the range of 10 mK to 1 K. For example, buffer-gas cooling methods have allowed for magnetic trapping of NH [17] and CaH [18] at ~ 1 K. The presence of the cooling He atoms naturally led to the studies of He-molecule collisions [19] and the observation of the quadratic dependence of the inelastic spin relaxation collision rate on rotational constant for $^3\Sigma$ NH molecules. Stark deceleration of supersonic molecular beams readily produces state-selected, ~ 100 mK samples at densities of 10^6–10^8 cm^{-3} [20,21]. Stark-decelerated molecules have been used in crossed-beam collisions with atomic species such as Xe [22].

In this Letter, we describe the confinement of cold dipolar molecules in a permanent magnetic trap loaded from a Stark decelerator. The open trap geometry facilitates molecular collision studies with external beams.

We present total collision cross sections for D_2-OH and He-OH collisions within a magnetic trap confining Stark-decelerated OH molecules. The atomic and molecular beams are produced in a supersonic nozzle cooled by liquid nitrogen, and the He-OH and D_2-OH center-of-mass collision energies can be tuned from 60 to 230 cm^{-1} and 145 to 510 cm^{-1}, respectively. To our knowledge, these energies represent the lowest observed in molecular collisions with absolute cross section measurements. Our magnetic trap design permits the application of electric dipole fields of tunable strength [23] that can be used to study novel dipolar collisions such as between fully polarized OH and NH_3. Both buffer-gas cooling [24] and Stark deceleration produce a large class of cold polar molecule beams. In combination with the trap described here, a wide variety of chemically interesting interspecies collisions can be studied at hitherto unexplored collision energies.

Importantly, collisions between hydrogen (H, H_2) and larger polar molecules (OH, H_2O, CO, H_2CO, SiO) are of astrophysical interest due to their possible role as pumps for interstellar masers [25]. In particular, specific emission lines of interstellar OH (1720 MHz) and H_2CO (4.8 GHz) masers have been attributed to collision-induced inversion by H_2 [26,27]. By directly comparing D_2-OH cross sections with those of the more theoretically tractable He-OH, we will aid molecular collision theory at energy scales below 200 cm^{-1}.

A pulsed supersonic beam of OH radicals is produced by striking an electric discharge through a mixture of 27 mbar H_2O and 1.5 bar Kr. The resulting OH beam consists of rotationally cold, $^2\Pi_{3/2}$ molecules whose mean longitudinal velocity is 490 m/s. The packet passes through a 3 mm diameter skimmer and is then coupled via an electrostatic hexapole into the 142-stage Stark decelerator. The Stark decelerator slows weak-field seeking OH molecules residing in the $|J = 3/2, m_J = \pm 3/2, f\rangle$ state, where J represents total angular momentum and m_J is the projection of J along the electric (E) field axis. The third quantum number denotes the parity of the state. The design and operating

principle of this decelerator is discussed in previous work [28]. The Stark decelerator is operated at a phase angle ϕ_0 of 50.352° in order to slow a 120 mK portion of the OH packet to 36 m/s. When slowing to velocities below 50 m/s, we observe maximum decelerator efficiency for $45° \leq \phi_0 \leq 55°$. Operation at these intermediate phase angles increases transverse packet confinement and reduces the coupling between transverse and longitudinal motion [29,30].

We stop and confine the decelerated 36 m/s OH packet within a permanent magnetic trap whose center lies 1 cm from the final decelerator rod pair. This trap, depicted in Fig. 1, represents a marked improvement over our previous magneto-electrostatic trap in both design simplicity and ultimate trapping efficiency [23]. The magnetic trap is constructed by mounting two Ni-coated NdFeB permanent ring magnets in an opposing orientation such that a magnetic quadrupole field is produced between them. The N42SH rating of these magnets ensures an operating temperature of up to 150 °C and a residual magnetization of 1.24 T. The inner and outer radii of the magnets measure 2 and 6 mm, respectively, while their thickness is 4 mm. The center-to-center magnet spacing of 7 mm in this magnetic trap yields a longitudinal magnetic (B) field gradient of 2 T/cm. This longitudinal separation matches the extent of the molecular packet entering the trap region from the Stark decelerator and therefore maximizes the trap density.

Figure 2 illustrates the trap loading sequence used with the magnetic trap of Fig. 1. In Fig. 2(a), the Ni coatings of the ring magnets are charged to ±12 kV precisely 1 μs after the final deceleration stage is grounded. At this point, the magnets become high-voltage electrodes and serve as a

final Stark-slowing stage for the 36 m/s molecules. In addition to the large stopping potential between the magnets, there exists a smaller potential between the final decelerator rod pair and the first trap magnet. This barrier reflects the small number of molecules with longitudinal velocity less than 25 m/s. However, the barrier's transverse E-field gradient serves to confine the slow molecules as they enter the trap region. The OH packet is brought to rest directly between the magnets in 400 μs, at which point the high voltage is switched off. Those hydroxyl radicals occupying the weak-magnetic-field-seeking $|3/2, 3/2, f\rangle$ state (50% of the stopped molecules) are then confined within a magnetic quadrupole trap measuring $k_B \times 480$ mK deep in the longitudinal dimension, where k_B is Boltzmann's constant. The trap potential is shown in Fig. 2(b). We note that Metsala *et al.* used a permanent magnet to reflect a molecular beam [31], but here we present the first realization of a permanent magnetic trap for neutral molecules.

Typical time-of-flight data and corresponding three-dimensional Monte Carlo simulation results are displayed in Fig. 3(a). Decelerated and trapped molecules are detected via laser-induced fluorescence (LIF). Lenses mounted in-vacuum allow for a fluorescence collection solid angle of ~0.1 sr. In Fig. 3(a), the large peak at 0.4 ms is the stopped OH packet imaged at trap center. Transverse oscillation of the trapped packet is observed in both data and simulation over 2 ms. The number and density of trapped OH are measured to be $>10^3$ and $\sim 10^6$ cm^{-3}, respectively. A temperature of 70 mK is estimated from Monte Carlo simulation, also consistent with the molecular packet delivered by the Stark decelerator. Because of the large quadrupole B field present in the trap, only a fraction of the OH sample is detected, as the longitudinal 5 GHz Zeeman shift near each magnet is larger than our LIF laser linewidth. This effect is included in the trap density estimates. Figure 3(b) displays the observed trap lifetime of 432 ± 47 ms, limited by colli-
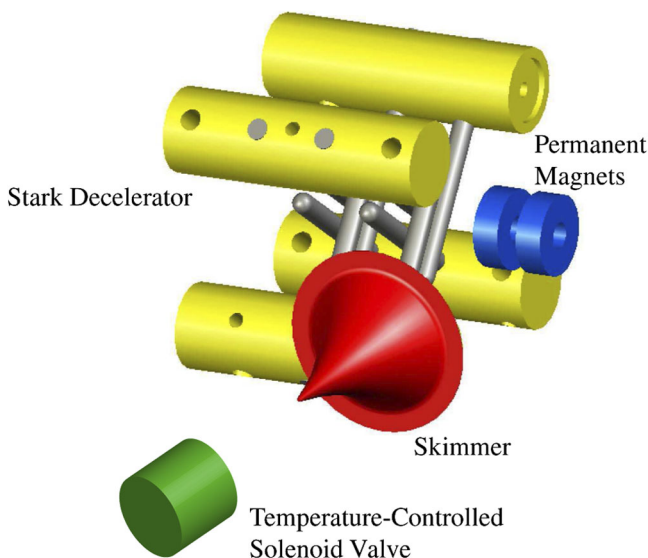

FIG. 1 (color online).   Illustration of the magnetic trap and pulsed valve assemblies. The foreground contains the temperature-controlled solenoid valve and 1 mm diameter skimmer. The final stages of the Stark decelerator and permanent ring magnets of the trap are shown in the background.

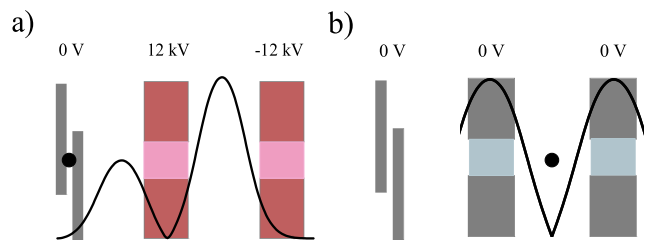

FIG. 2 (color online).   Illustration of the trap loading sequence. (a) High voltage is applied to the surfaces of the two permanent ring magnets 1 μs after the final deceleration stage (shown at left) is grounded. The OH packet is stopped directly between the two magnets by the electric field gradient in 400 μs. The stopping potential due to the applied electric field is depicted. (b) The magnet surfaces are electrically grounded, leaving the packet trapped within the displayed permanent magnetic quadrupole potential.
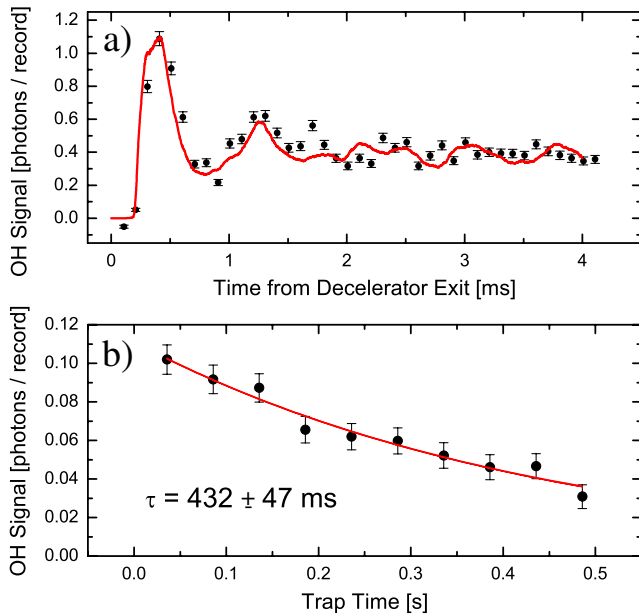
FIG. 3 (color online).   (a) Time-of-flight data (circles with error bars) and three-dimensional Monte Carlo simulations (solid line) corresponding to OH trap loading. Stopping E fields are switched off at 0.4 ms, which leaves 50% of the stopped OH molecules trapped in the permanent magnetic quadrupole. (b) Measurement of the lifetime of OH trapped within the magnetic trap at a background pressure of 7.5×10^{-9} Torr. A single-exponential fit (solid line) of the data yields 432 ± 47 ms.

sions with background gas. The trap chamber pressure of 7.5×10^{-9} Torr consists of equal parts H_2O and Kr. We note that this trap would be ideal for proposed multiple-loading schemes for molecules such as NH [32].

The open structure of the magnetic trap allows for low center-of-mass energy ($E_{c.m.}$) collision studies between the trapped OH and external molecular or atomic beams. As large electric fields are used only for initial trap loading, there is no risk of high-voltage breakdown when pulsing such beams through the trap. Furthermore, though all collisions reported herein were observed with the magnets grounded, a relatively small polarizing E field (few kV/cm) can be applied to the magnets after trap loading without loss of confined molecules—thereby enabling investigation of dipolar collisions. Figure 4 displays results from separately scattering beams of He and D_2 with the trapped OH sample. For this work, we place a pulsed solenoid valve (General Valve Series 99) and 1 mm diameter skimmer assembly, as shown in Fig. 1, such that the skimmed atomic or molecular beam passes directly between the magnets. The solenoid valve rests in a bath of liquid nitrogen while its 1 mm output nozzle is heated via 25 turns of manganin wire to allow for tuning of the beam velocity. All scattering data are taken at He and D_2 backing pressures of 2.0 and 2.7 bar, respectively. As expected, we observe that the beam velocities scale as the square root of the nozzle temperature. The $E_{c.m.}$ of the He-OH and
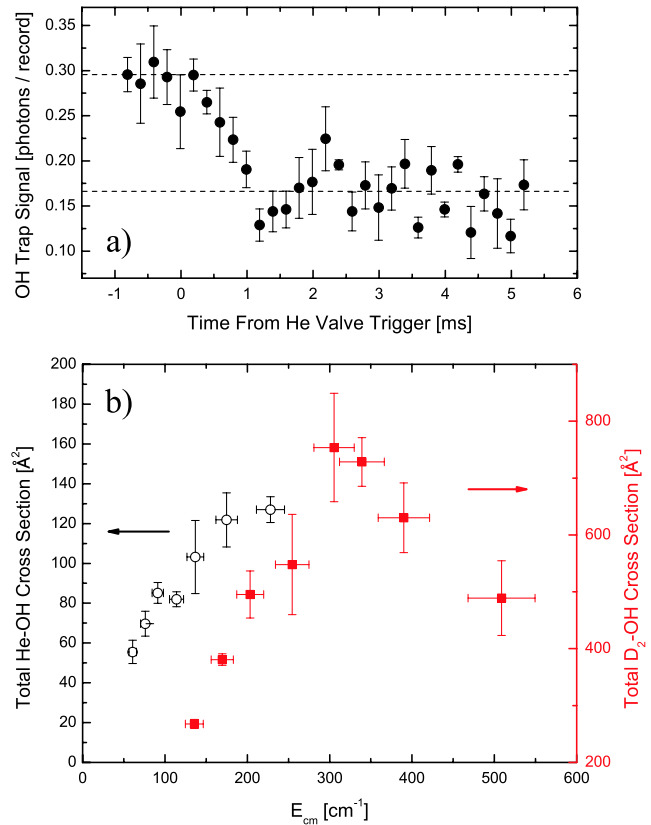

FIG. 4 (color online).   (a) Time dependence of OH trap loss due to collisions with a supersonic He beam. Trap density drops sharply over 1 ms upon He beam collisions, then remains constant over the time scale shown. The valve is triggered 20 ms after the magnetic trap is loaded. (b) Total collision cross sections for He-OH (open circles) and D_2-OH (squares) as a function of $E_{c.m.}$. The decrease in the He-OH cross section at low energy is attributed to reduced inelastic loss as $E_{c.m.}$ drops below the 84 cm^{-1} splitting between the $J = 3/2$ and $J = 5/2$ states of the OH molecule.

D_2-OH systems can therefore be tuned to minima of ~60 cm^{-1} and ~145 cm^{-1}, respectively. Measurements of beam flux and velocity are made using a fast ionization gauge and a microphone-based pressure sensor placed 13 cm apart. The uncertainty in the interspecies calibration of the ionization gauge is ~10%. The measured 8% velocity spread of the supersonic He beam gives a collision energy resolution of 9 cm^{-1} at the lowest nozzle temperature.

Figure 4(a) displays the time dependence of OH trap loss as a supersonic beam of He traverses the magnetic trap. Trap density drops sharply over the first ~1 ms after the solenoid valve is fired, then remains constant over the time scale shown. Although the partial pressure of the scattering gas in the trap chamber rises as the supersonic beam scatters from the chamber walls, we measure an OH trap lifetime of >50 ms following the initial collision. Such vastly different time scales allow us to differentiate be-

tween trap loss due to the supersonic beam and that result-
ing from background gas collisions. Trap loss at a given
nozzle temperature is measured by repeatedly comparing
OH population 1 ms *before* and 2 ms *after* the solenoid
valve is triggered. The total cross sections of Fig. 4(b) are
determined from the trap loss data by normalization to the
corresponding beam flux measured with the fast ionization
gauge at a given nozzle temperature. We also find that the
trap loss scales linearly with the beam flux, confirming that
we are operating in the single-collision regime.

An important advantage inherent to using trapped mole-
cules as the scattering target is the ability to directly
measure the absolute collision cross section. To do this,
we use a leak valve to fill the trap chamber with a known
pressure of He gas, then measure the OH trap lifetime at
that pressure. The temperature of the chamber walls is
298 K, placing the $E_{c.m.}$ of the thermal He-OH collisions
at ~ 250 cm^{-1}. The data point for He-OH collisions at
230 cm^{-1} from Fig. 4(b) is then scaled to this absolute
cross section of 127 ± 18 Å^2.

For OH molecules in their ground electronic and vibra-
tional state, the energy splitting of the two lowest lying
rotational levels, $J = 3/2$ and $J = 5/2$, is 84 cm^{-1}. In a
previous crossed-beam experiment, an abrupt decrease in
the Xe-OH inelastic cross section was observed as $E_{c.m.}$
was tuned below this value [22]. The He data of Fig. 4(b)
possess this feature. Because the magnetic trapping poten-
tial is sensitive to the internal state of the OH molecule, we
cannot differentiate between trap loss due to elastic or
inelastic collisions. Nevertheless, such a sudden decrease
of the total cross section below 84 cm^{-1} is indicative of
threshold behavior. The collision cross section of D_2-OH is
larger than that of He-OH. This is understandable since the
D_2 beam is an ortho-para mixture and contains a large
fraction of frozen-in $J = 1$ population. The ratio of the
two cross sections at 230 cm^{-1} is consistent with previous
H_2-OH and He-OH pressure-broadening measurements
made at a temperature of 298 K [33]. The enhanced colli-
sion cross sections for D_2-OH result from the quadrupole
moment of the D_2 $J = 1$ state that can interact strongly at
long range with the OH dipole. Yet another striking feature
of the collision data is the pronounced peak in the D_2-OH
cross section for $E_{c.m.} \sim 305$ cm^{-1}, which suggests reso-
nant energy transfer. Although more theoretical considera-
tion is warranted, the 300 cm^{-1} $J = 3 \leftarrow J = 1$ transition
of the $^1\Sigma_g^+$ D_2 molecule may be contributing to the inelas-
tic cross section at this energy. Another possible explana-
tion is collision-induced decay of $J = 2$ molecules present
in an imperfect D_2 supersonic expansion.

In conclusion, we demonstrate a new permanent mag-
netic trap design that confines a dense sample of cold OH
molecules as a cold collision target. Velocity-tunable
supersonic beams of He and D_2 intersecting the magneti-
cally trapped cold OH molecules yield absolute collision

cross sections over an energy range of 60 to 230 cm^{-1} and
145 to 510 cm^{-1}, respectively. Threshold behavior is ob-
served in He-OH collisions, and an enhancement of inelas-
tic cross sections is seen in the D_2-OH system near
305 cm^{-1}. Having demonstrated the usefulness of this
permanent magnetic trap for collision studies, future goals
include using colder continuous beams of polar molecules
as the colliding partner for OH. With the ability to apply a
sufficiently strong polarizing field within the magnetic trap
[34], we aim to reach sufficiently low $E_{c.m.}$ to observe
dipole-dipole interactions.

[1] J. J. Hudson *et al.*, Phys. Rev. Lett. **89**, 023003 (2002).
[2] E. R. Hudson *et al.*, Phys. Rev. Lett. **96**, 143004 (2006).
[3] B. L. Lev *et al.*, Phys. Rev. A **74**, 061402(R) (2006).
[4] A. Micheli *et al.*, Nature Phys. **2**, 341 (2006).
[5] R. V. Krems, Int. Rev. Phys. Chem. **24**, 99 (2005).
[6] E. R. Hudson *et al.*, Phys. Rev. A **73**, 063404 (2006).
[7] L. Santos *et al.*, Phys. Rev. Lett. **85**, 1791 (2000).
[8] A. V. Avdeenkov *et al.*, Phys. Rev. A **69**, 012710 (2004).
[9] K. Goral *et al.*, Phys. Rev. Lett. **88**, 170406 (2002).
[10] S. Yi *et al.*, Phys. Rev. Lett. **93**, 040403 (2004).
[11] T. Kohler *et al.*, Rev. Mod. Phys. **78**, 1311 (2006).
[12] K. M. Jones *et al.*, Rev. Mod. Phys. **78**, 483 (2006).
[13] J. J. Zirbel *et al.*, Phys. Rev. Lett. **100**, 143201 (2008).
[14] E. R. Hudson *et al.*, Phys. Rev. Lett. **100**, 203201 (2008).
[15] J. Sage *et al.*, Phys. Rev. Lett. **94**, 203001 (2005).
[16] K. K. Ni *et al.*, Science **322**, 231 (2008).
[17] W. C. Campbell *et al.*, Phys. Rev. Lett. **98**, 213001
      (2007).
[18] J. Weinstein *et al.*, Nature (London) **395**, 148 (1998).
[19] W. C. Campbell *et al.*, arXiv:0804.0265v1.
[20] H. L. Bethlem *et al.*, Phys. Rev. Lett. **83**, 1558 (1999).
[21] J. Bochinski *et al.*, Phys. Rev. Lett. **91**, 243001 (2003).
[22] J. J. Gilijamse *et al.*, Science **313**, 1617 (2006).
[23] B. C. Sawyer *et al.*, Phys. Rev. Lett. **98**, 253002 (2007).
[24] D. Patterson and J. M. Doyle, J. Chem. Phys. **126**, 154307
      (2007).
[25] M. Elitzur, Rev. Mod. Phys. **54**, 1225 (1982).
[26] J. Guibert *et al.*, Astron. Astrophys. **66**, 395 (1978).
[27] I. M. Hoffman *et al.*, Astrophys. J. **598**, 1061 (2003).
[28] J. Bochinski *et al.*, Phys. Rev. A **70**, 043410 (2004).
[29] S. Y. T. van de Meerakker *et al.*, Phys. Rev. A **73**, 023401
      (2006).
[30] B. C. Sawyer *et al.*, Eur. Phys. J. D **48**, 197 (2008).
[31] M. Metsala *et al.*, New J. Phys. **10**, 053018 (2008).
[32] S. Y. T. van de Meerakker *et al.*, Phys. Rev. A **64**, 041401
      (R) (2001).
[33] K. Park *et al.*, J. Quant. Spectrosc. Radiat. Transfer **55**,
      285 (1996).
[34] R. V. Krems, Phys. Rev. Lett. **96**, 123202 (2006).